

Examining the gastrointestinal transit of lipid-based liquid crystalline systems using whole-animal imaging

Anna C. Pham¹ · Tri-Hung Nguyen¹ · Cameron J. Nowell² · Bim Graham³ · Ben J. Boyd^{1,4}

Published online: 2 September 2015
© Controlled Release Society 2015

Abstract Lipid-based liquid crystalline (LC) systems have the potential to sustain the oral absorption of poorly water-soluble drugs in vivo, facilitating slow drug release from their complex internal structure. To further evaluate the dynamic relationship between gastric retention and sustained drug absorption for these systems, this study aimed to explore non-invasive X-ray micro-CT imaging as an approach to assess gastric retention. Pharmacokinetic studies were also conducted with cinnarizine-loaded LC formulations to correlate gastric retention of the formulation to drug absorption. The in vivo studies demonstrated the interplay between gastric retention and drug absorption based on the digestibility of the LC structures. An increase in non-digestible phytantriol

(PHY) composition in the formulation relative to digestible glyceryl monooleate (GMO) increased the gastric retention, with 68 ± 4 % of formulation intensity remaining at 8 h for 85 % w/w PHY, and 26 ± 9 % for 60 % w/w PHY. Interestingly, it was found that PHY 30 % w/w in GMO provided the highest bioavailability for cinnarizine (CZ) amongst the other combinations, including GMO alone. The studies demonstrated that combining digestible and non-digestible lipids into LC systems allowed for an optimal balance between sustaining drug absorption whilst increasing plasma concentration (C_{\max}) over time, leading to enhanced oral bioavailability. The results demonstrate the potential for utilising non-invasive X-ray micro-CT imaging to dynamically assess the GI transit of orally administered liquid crystal-forming formulations.

Electronic supplementary material The online version of this article (doi:10.1007/s13346-015-0253-z) contains supplementary material, which is available to authorized users.

✉ Tri-Hung Nguyen
tri-hung.nguyen@monash.edu

✉ Ben J. Boyd
ben.boyd@monash.edu

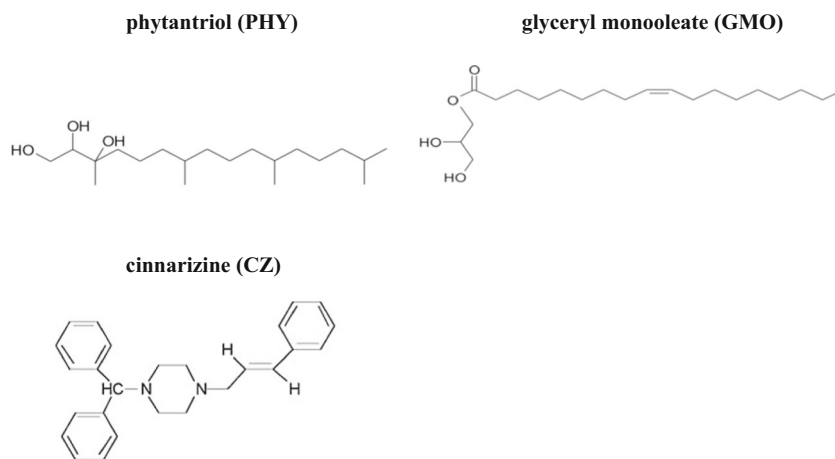
- ¹ Drug Delivery Disposition and Dynamics - Monash Institute of Pharmaceutical Sciences, Monash University (Parkville Campus), 381 Royal Parade, Parkville, Victoria 3052, Australia
- ² Drug Discovery Biology - Monash Institute of Pharmaceutical Sciences, Monash University (Parkville Campus), 381 Royal Parade, Parkville, Victoria 3052, Australia
- ³ Medicinal Chemistry - Monash Institute of Pharmaceutical Sciences, Monash University (Parkville Campus), 381 Royal Parade, Parkville, Victoria 3052, Australia
- ⁴ ARC Centre of Excellence in Convergent Bio-Nano Science and Technology, Monash Institute of Pharmaceutical Sciences, Monash University (Parkville Campus), 381 Royal Parade, Parkville, Victoria 3052, Australia

Keywords Liquid crystalline · Sustained release · Phytantriol · Glyceryl monooleate · X-ray computed tomography · Gastrointestinal transit · Oral drug delivery

Introduction

Phytantriol (PHY) and glyceryl monooleate (GMO) (Fig. 1) are examples of two amphiphilic lipids that form a cubic liquid crystalline (LC) phase in excess water and are currently being investigated as sustained drug delivery vehicles [1–5]. Recent studies assessing the oral bioavailability and gastrointestinal disposition of PHY and GMO formulations containing cinnarizine (CZ) (Fig. 1) in rats reported that the PHY formulation was retained in the stomach longer compared to the equivalent GMO formulation [1]. Subsequent pharmacokinetic (PK) studies showed a correlation between the gastric retention of the formulations and sustained absorption of CZ, with the PHY-based formulation sustaining drug absorption

Fig. 1 Chemical structures of phytantriol (PHY), glycerol monooleate (GMO) and cinnarizine (CZ)



for longer than GMO. The reduced gastric retention of the GMO formulation, and consequent faster absorption of CZ, was attributed to the increased digestibility of GMO, due to the susceptibility of the ester linkage to acid-catalysed hydrolysis and enzymatic degradation (Fig. 1) resulting in loss of the viscous LC structure. Despite its limited gastric retention, GMO still possessed some physicochemical and pharmacokinetic benefits when compared to PHY, including a higher drug solubilising capacity [2] and significantly higher plasma concentration (C_{max}) when co-administered with CZ, consistent with previous studies [6]. The contrasting PK response from both formulations therefore suggests the potential to modulate drug absorption using varying compositions of these two lipids.

The hypothesis driving the current study was that co-formulation of CZ with mixtures of PHY and GMO may allow for sustained absorption brought about by the PHY in addition to high CZ plasma concentrations and enhanced bioavailability, as a result of the presence of the GMO. To date, the gastrointestinal retention and absorption behaviour of drug from such combined lipid formulation vehicles has yet to be reported. Therefore, this study aims to further understand the *in vivo* behaviour of these lipid-based systems by assessing the gastric retention of the formulations comprising varying compositions of PHY and GMO in rats with pharmacokinetic studies subsequently conducted to correlate retention with drug absorption for the chosen compositions.

Previous studies of gastric retention of LC formulations have taken an analytical approach of sacrificing cohorts of animals at fixed time points and assaying gastric contents [2, 7]; however, developments in *in vivo* imaging now allow alternate approaches to be applied to such studies. Hence, a second aim of this study was to determine the potential of X-ray computed tomography (CT) imaging for serial imaging of the disposition of formulations in the GIT. Given the advantages of using gold as a contrasting agent [8, 9], gold nanoparticles (GNP) were incorporated into the lipid formulations for monitoring the dynamic transit of various lipid-based LC

formulations to assess gastric retention. The effect of GNP on the phase behaviour of the liquid crystalline systems was evaluated. The gastric retention of the liquid crystal-forming lipid systems was compared to that of tributyrin as a digestible lipid that does not form liquid phases and to GNPs alone.

Materials and methods

Materials

Phytantriol (PHY), 3,7,11,15-Tetramethylhexadecane-1,2,3-triol, was purchased from DSM Nutritional Products (Singapore), with a minimum purity of 95 %. Myverol 18–99 K was purchased from Kerry Ingredients (Norwich, USA) and was used as a substitute for glycerol monooleate (60.9 % purity) as it possesses similar phase behaviour [10]. Tributyrin was purchased from TCI Chemicals (Tokyo, Japan). All lipids were used without further purification. Gold chloride (III) ($AuCl_3$) and tri-sodium citrate di-hydrate, potassium chloride, cinnarizine (CZ) and diazepam, and formic acid (MS grade) were purchased from Sigma-Aldrich (St. Louis, USA) and sodium citrate APS Ajax Finechem (Auburn, Australia). Hydrochloric acid (AR) and acetonitrile (HPLC analysis grade) were purchased from (Merck, Australia). Lethabarb (325 mg/mL pentobarbitone sodium) was purchased from Abbott Laboratories Pty. Ltd. (NSW, Australia). Di-sodium hydrogen orthophosphate and potassium dihydrogen orthophosphate were purchased from APS Ajax Finechem (Auburn, Australia); sodium chloride was purchased from Chem-Supply, Australia. Milli-Q water used was obtained from a Millipore water purification system (Billerica, USA).

Sample preparation

The method of preparation of gold nanoparticles is provided in the [electronic supplementary information](#). Prior to mixing with PHY and/or GMO, 1.5 mL aliquots of GNP suspension

(equivalent to 0.405 mg of GNP, assuming 100 % yield) were centrifuged at $12,470\times g$ for 30 min at room temperature to produce a GNP pellet. The supernatant layer containing dissolved salts was then removed, and the GNP pellet was redispersed in 100 μL of Milli-Q water. The redispersed GNP suspension was then added to 200 mg of lipid, and the mixture was freeze dried using a Virtis AdVantage 2.0 BenchTop Freeze Dryer/Lyophilizer by SP Scientific (Warminster, PA) for 1 day to produce a suspension of GNP in lipid. Phosphate-buffered saline (PBS; pH 2 or 8) was then added to the lipid, heated to 60 °C for 5 min and vortexed for 1 min. The heating and mixing process was repeated twice. The bulk sample was then placed on a roller mixer at 37 °C to equilibrate for 24 h. Samples containing GMO were prepared 1 day in advance prior to small-angle X-ray scattering (SAXS) analysis as the lipid was susceptible to hydrolysis at both high (pH 8) or low (pH 2) pH.

Small-angle X-ray scattering

Determination of phase structure using SAXS was conducted at the SAXS/WAXS beamline at the Australian Synchrotron facility [11]. Samples were placed into 96-well Corning microplates, sealed with an adhesive cover, heated to 37 °C in an oven and analysed using X-rays at a wavelength of 1.1271 Å (11 keV). The total q range was $0.03 < q < 1.68/\text{\AA}$, with a sample-to-detector distance of 567 mm. 2D SAXS patterns were obtained with a 2-s exposure using a Pilatus 1M detector. The custom software package ScatterBrain (V. 2.10) was used to integrate the 2D patterns to 1D intensity vs. q profiles, which were then used to determine phase structures using known peak positions for different structures [12].

X-ray micro-CT imaging

Imaging procedure

All animal studies conducted were approved by the Monash Institute of Pharmaceutical Sciences Animal Ethics Committee. Male Sprague-Dawley rats (280–320 g) were used for the imaging studies. The animals were transferred to individual metabolism cages and fasted for at least 12 h prior to dosing to ensure residual food did not influence the X-ray contrast. However, water was provided ad libitum. X-ray CT imaging was conducted on a nanoCT by Mediso Medical Imaging Systems (Budapest, Hungary). At each imaging time point, rats were first anaesthetised with isoflurane (5 % v/v) (and maintained at 1.5 % v/v throughout the imaging procedure) and placed in a feet first-prone position tube holder within the micro-CT instrument. A scout view was taken, with a tube voltage of 45 kVp and exposure time of 1100 ms, followed by a helical scan with the zoom set on medium, with

180 projections, pitch of 1, tube voltage of 45 kVp, exposure time of 1100 ms and binning of 1:4. Post-reconstructions of the scans were carried out with a resolution of 76.8916 μm in each dimensions (isotropic scans). The duration of the helical scan was approximately 9 min. After the pre-dose scan, each rat was briefly removed from the sample holder and whilst still unconscious, the formulation (300 mg) was administered via oral gavage. The rat was immediately returned and repositioned into the holder (maintained under 1.5 % v/v isoflurane) and the post-dose scan was performed. After the pre- and post-dose scans, rats were returned to their individual metabolism cages to recover from anaesthesia under a heat lamp. The scanning process was repeated at 1, 2, 4, 6 and 8 h with the rat allowed to recover between scans. Imaging for each formulation was performed in triplicate ($n=3$).

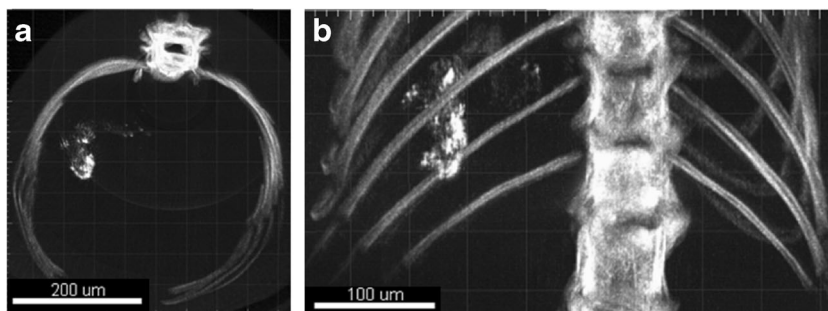
Analysis of imaging results

Results were analysed using Imaris software by Bitplane (Zurich, Switzerland) for 3D data visualisation and quantification of the GI transit of the examined formulations. Gamma settings were reduced to 0.4 to qualitatively remove background noise and artefacts. As the high density of bone and heavy tissue (e.g. spinal cord) can cause high attenuation of X-rays, intensity and volume measurements were taken from two vertebrae directly above and one below the last floating rib of each (total of four vertebrae). This resulted in minimal contribution from these artefacts and improved the contrast of the gastric region (Fig. 2). Gastric regions were pre-determined from initial dissection of the rat's lower thorax and abdomen region in a separate cohort of rats of similar size and weight to those used in the imaging study.

A virtual core to define the volume for quantitation was manually inserted by drawing within the rib and the spinal cord of the rat through the imaged slices as demonstrated in Fig. 3. All contrast signals outside the core (spine and ribs) were then set to 0 to remove interference. The area within the core was then calculated for intensity and volume, with the calculated contrasts highlighted in green (Fig. 4). Highlighted components on the opposite side of the stomach (small intestine region)—components past the middle of the spine and rib cage, were manually removed and excluded from the intensity and volume calculations. This allowed for gastric retention of the formulations to be exclusively quantitated without interference.

When quantifying the core, the surface grain size was reduced to 1 μm and the threshold limit was increased to 13,000 to reduce background noise from being included as contrast produced from the retention of the formulation. The total sum of intensity values and total volume within the core were obtained and collated to assess the sum of intensity and volume remaining over time.

Fig. 2 **a** Example of cropped sagittal 6 view and **b** front view of the gastric region of rat administered the GNP+PHY/GMO 60:40, at 2 h after administration



Pharmacokinetic studies

Preparation of formulations for PK studies

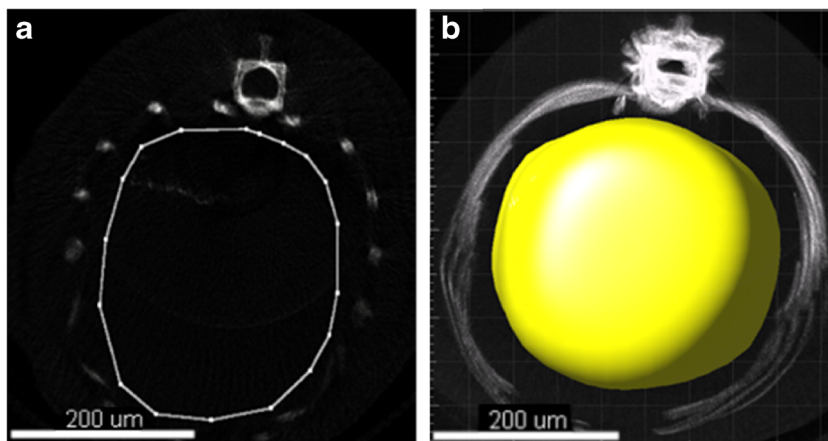
To prepare drug-loaded lipid formulations, CZ was added to molten PHY/GMO mixtures at a drug loading of 7 mg/g and allowed to equilibrate overnight at 37 °C to ensure the CZ was fully dissolved into the formulation. Pharmacokinetic studies were conducted using a separate cohort of male Sprague-Dawley rats (270–310 g, $n=3$ per dose group), to that used in the imaging studies. To facilitate serial blood collection, rats were anaesthetised via inhalation of isoflurane (5 % v/v , and maintained at 2 % w/w for duration of the surgical procedure) and the right carotid artery cannulated with polyethylene tubing (0.96 mm o.d \times 0.58 mm i.d. Microtube Extrusions, NSW) and allowed to recover overnight prior to dose administration. Rats were also fasted for 12 h prior to and 8-h post dosing with water provided. To each animal, 300 mg of formulation (equivalent to a dose of 7 mg/kg CZ per 300 g rat) was administered via oral gavage. Blood samples (250 μ L) were collected at 0, 0.5, 1, 2, 3, 4, 6, 8, 10 and 24 h after dosing and transferred to 1.5 mL microcentrifuge tubes containing 10 IU sodium heparin. The cannula was also flushed with 10 IU/mL heparin in normal saline between time points to maintain patency. Blood samples were centrifuged at 6700 \times g for 5 min and 50 μ L plasma aliquots collected and transferred to microcentrifuge tubes. Plasma

samples were stored at -20 °C until required for the assay for CZ content.

Analysis of CZ in plasma

Plasma samples were assayed using a LC-MS/MS system comprising a Waters ACQUITY H-Class ultra performance liquid chromatography (UPLC) system, coupled to a TQ-S tandem mass spectrometer (MS/MS) (Waters, Milford, MA). A Supelco Ascentis Express RP Amide column (2.7 μ m, 50 \times 2.1 mm) (St. Louis, USA) and Phenomenex SecurityGuard Cartridge C₁₈ guard column (Phenomenex, Torrance, CA) was connected to an UPLC pump, autosampler with the column heater maintained at 40 °C. Analysis was performed on a TQ-S MS/MS system comprising an electron spray ionisation probe set on positive ionisation mode with capillary set at 3.68 kV. The multiple reaction monitoring (MRM) for CZ transition was from m/z 369.21 > 167.11, with the cone voltage and collision energy set to 31 V and 24 eV, respectively. CZ was eluted at 2.29 min and the internal standard, diazepam at 2.63 min. Desolvation gas temperature was set at 200 °C with a flow rate of 900 L/h. The multiple reaction monitoring (MRM) and total ion scans to detect diazepam in plasma samples were m/z 285.2 > 154.0 with a cone voltage of 33 V and collision energy of 19 eV. The mobile phase was set at 0.5 mL/min and consisted of component A: Milli-Q containing 0.05 % (v/v) formic acid and B: Acetonitrile containing

Fig. 3 **a** Example manual insertion of a core at a single slice and **b** sagittal 6 view and front view of a new surface added within the spine and rib cages on Imaris



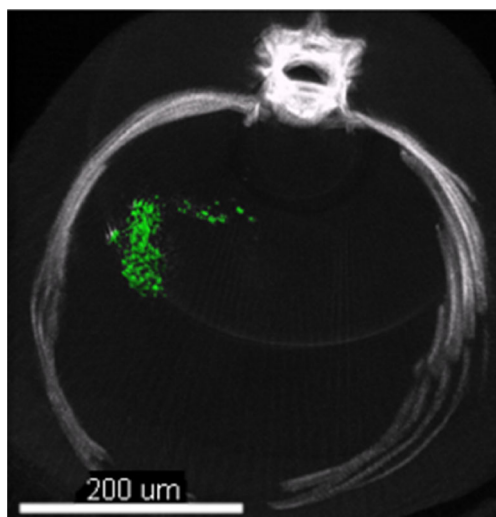


Fig. 4 Example of surface contours added into contrast to outline calculated region

0.05 % (v/v) formic acid. The mobile phase was delivered over 4 min via the following gradient: 0–0.15 min (2 % B), 0.15–0.2 min (2–10 % B), 0.2–2.5 min (10–80 % B), 2.5–2.8 min (80–95 % B), 2.8–3.3 min (95 % B), 3.3–3.5 min (95–2 % B) and 3.5–4.0 min (2 % B). Run time was 4 min, with the injection volume at 2.5 μ L.

Results

Effect of GNP on phase behaviour of lipids in aqueous media

All GMO and PHY mixtures retained the cubic Pn3m-type structure with the addition of GNP; there was no significant change indicated by the clear spacing ratios between the peaks at $\sqrt{2}$, $\sqrt{3}$, $\sqrt{4}$, $\sqrt{6}$, $\sqrt{8}$ and $\sqrt{9}$ (Supplementary Info Fig. S1), with a slight decrease in the calculated lattice parameter with increasing concentrations of GNP (0, 1, 2 and 5 %) for the PHY-only systems (Fig. 5). In contrast, a slight but not significant increase in lattice parameters was observed with increasing concentrations of GNP (0, 1, 2 and 5 %) for the GMO-only systems at pH 2 compared to pH 8. Overall, the LC structure formed was therefore not significantly influenced over the GNP concentration studied.

Gastric retention of lipid formulations and GNP from X-ray CT imaging

The amount of lipid remaining over time for varying compositions of PHY and GMO and controls are shown in Fig. 6. X-ray contrast observed for the mixed systems was generally less intense compared to 100 % PHY, whilst for GMO and the

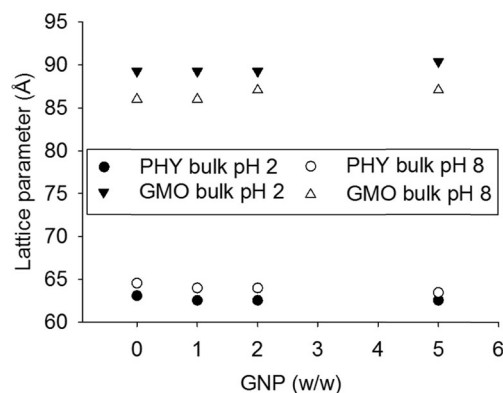


Fig. 5 Lattice parameter of cubic phases formed by PHY and GMO bulk systems on concentration of gold nanoparticles up to 5 % w/w

negative controls, GNP suspension and tributyrin (TB), there was little or no contrast detected at the 4 or 8 h time points.

Based on the calculated sum of intensity and volume at 8 h after oral administration, gastric retention was greatest with 100 % PHY, with the highest amount of lipid remaining at 8 h (Fig. 7). A general trend was also observed, where an increase in GMO content relative to PHY resulted in a decrease in gastric retention. However, due to some inter-subject variability within groups, the differences at 8 h after administration were not significant (see Supplementary Information Table S1 and S2 for the total percentage of intensity and volume remaining and the collated values for lipid remaining over time, and Table S3 for statistical analysis of the imaging results). Although the results were considered semi-quantitative, they nevertheless allowed for each formulation to be clearly ranked from the most retained to the least retained, and therefore supported the hypothesis where an increase in PHY content induced a corresponding increase in gastric retention.

Pharmacokinetic studies

The previously determined plasma profiles for 100 % PHY and 100 % GMO formulations are reproduced in Fig. 8 [2], showing that the plasma concentrations for CZ dropped rapidly to baseline for GMO, whilst a significantly sustained profile was apparent for the PHY formulation. For the mixtures of PHY and GMO, the plasma profiles for the formulations were all similar (Fig 8) and fell between those of 100 % PHY and GMO in the first 10 h. The profiles for the combined PHY and GMO trended towards higher values for C_{max} compared to 100 % PHY, suggesting the increase in GMO content induced an increase in C_{max} .

The pharmacokinetic parameters for CZ when administered in each formulation are summarised in Table 1. All combinations of PHY with GMO exhibited an increasing trend in AUC for CZ relative to both 100 % PHY and 100 % GMO formulations over 24 h. Formulations comprising higher

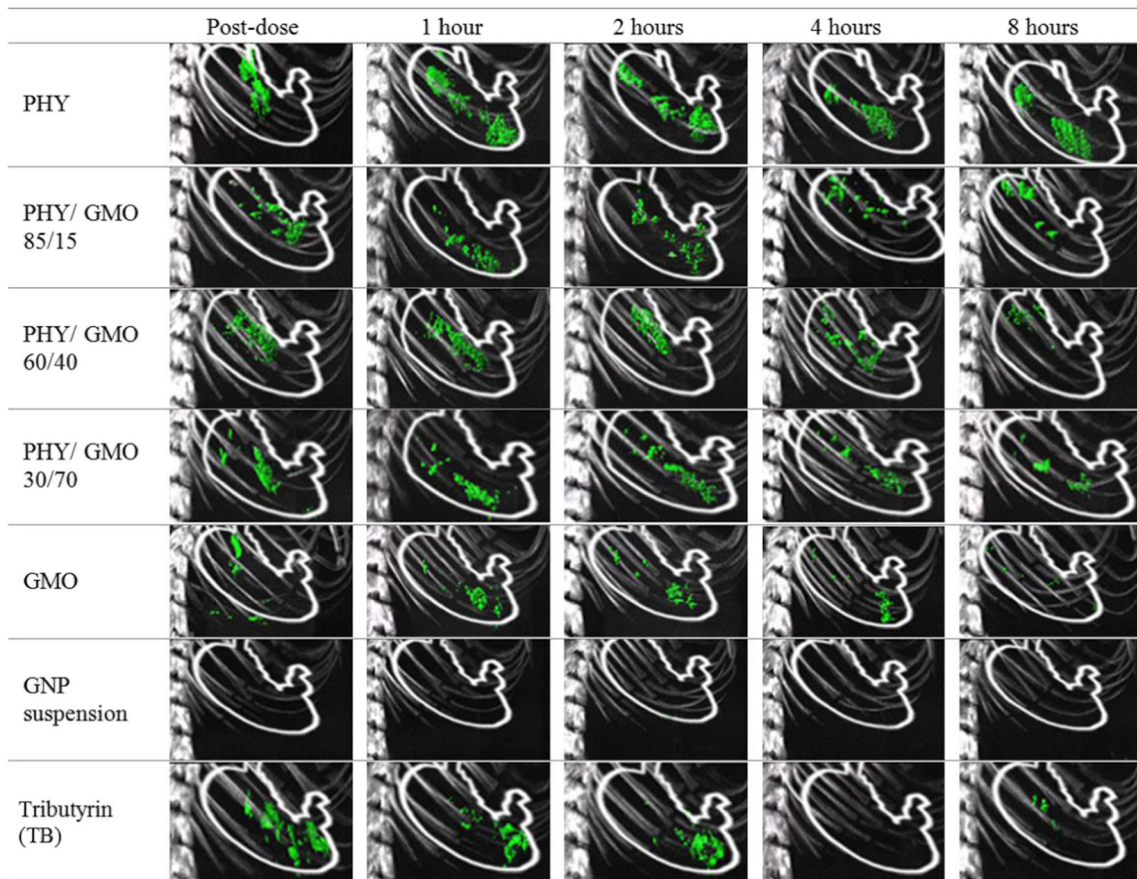


Fig. 6 Side view of the gastric compartment of rats dosed with the seven formulations, containing 5 % w/w GNP imaged over 8 h. The stomach outline is used as an anatomical guide only and may not necessarily

reflect the true outline of the stomach. Appearance of some contrast at 8 h for tributyrin (*TB*) was potentially attributed to rats being coprophagic. However, beyond 2 h, there was no or minimal contrast observed

proportions of GMO resulted in a higher AUC, greater than that of GMO alone after 24 h; however, only the PHY 30 % formulation exhibited a significant increase in AUC (1473 ± 94 ng/mL.h) compared to 100 % PHY ($p < 0.05$). The AUC

was observed to be the highest with the PHY 30 % formulation, followed by PHY 60 % formulation, PHY 85 % formulation, 100 % GMO, then 100 % PHY. Note that AUC was

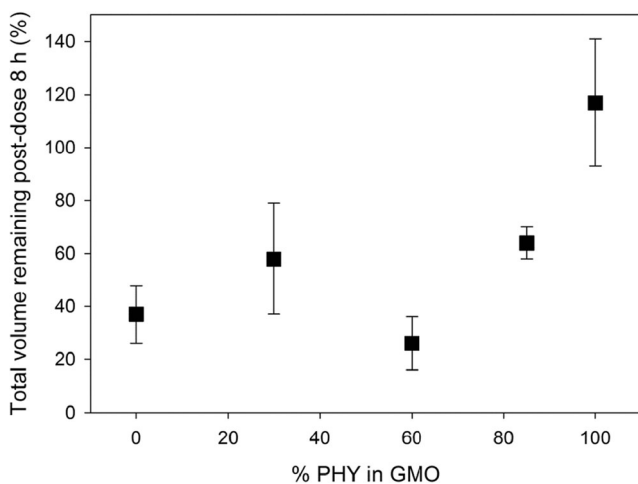


Fig. 7 Mean normalised percentage of sum of intensity remaining 8 h after administration of the PHY/GMO combinations illustrated in Fig. 6 (data are mean \pm SEM, $n=3$); 0 % PHY indicates 100 % GMO

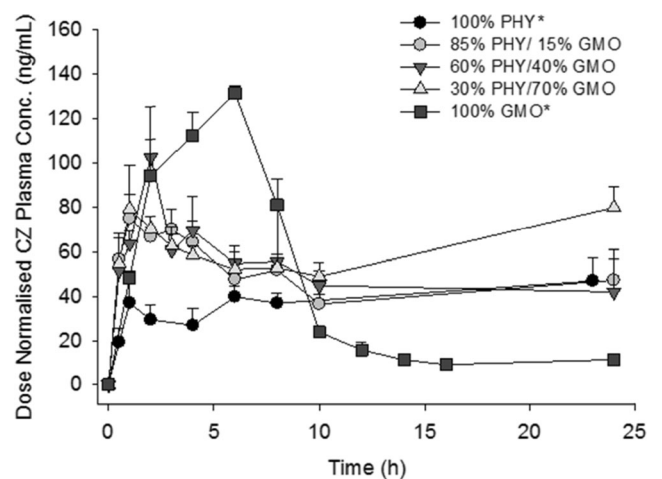


Fig. 8 Dose normalised CZ plasma concentration after administration in various PHY/GMO combinations, dosed via oral gavage in rats (mean \pm SEM, $n=3$). Lines were used to calculate AUC and do not necessarily represent true CZ plasma concentrations between time points. *100 % PHY and 100 % GMO PK data were obtained from Nguyen et al. [2]

Table 1 Pharmacokinetic parameters for cinnarizine after administration in the various PHY and GMO mixtures in rats

	PHY*	PHY/GMO 85:15	PHY/GMO 60:40	PHY/GMO 30:70	GMO*
C_{\max} (ng/mL)	46.9±10.5*	79±6.8*	102±23	88±14	134±3.6*
T_{\max} (h)	9.5±4.7	1.2±0.4	2±0.0	1.3±0.3	5±1
AUC 0– T_{last} (ng/mL.h)	880±139**	1137±169	1213±102	1473±94**	1045±16

Values are provided as mean±SEM, $n=3$

* $p<0.05$ for GMO between PHY and PHY/GMO 85:15, which are similar

** $p<0.05$ for the AUC between PHY/GMO 30:70 and PHY alone. See [supplementary information](#) for the ANOVA one-way post hoc Tukey multiple comparisons statistical analysis of the AUC, C_{\max} and T_{\max} . Shaded cells indicate data obtained from Nguyen et al. 2010 [2]

truncated to 23 h for 100 % PHY and T_{last} for 100 % GMO PK profiles obtained from Nguyen et al. [2].

Discussion

X-ray micro-CT imaging has been demonstrated in this study to be a useful technique for examining the gastrointestinal transit of lipid-based LC systems. However, inter-subject variability within dosing groups combined with some complications with the imaging analysis makes it difficult to demonstrate statistically significant differences from the images quantitatively at this stage. Nevertheless, visual examination of the trends in the images in Fig. 6 and the mean normalised percentage of sum of intensity remaining after 8 h in Fig. 7, allowed for semi-quantitative interpretation of the formulations.

GNP as a contrasting agent for assessing the gastric disposition of lipid formulations

The addition of 5 % (w/w) GNP into PHY and GMO LC systems provided sufficient contrast for comparing gastric retention between PHY and GMO and did not result in any significant change to the LC structure or the lattice parameter as shown in Fig. 5. This is consistent with a recent report by Du et al. using the GNPs as photothermal elements for remote near-infrared heating of liquid crystalline structures [13] and may be due to the hydrophilic nature of the chosen GNP, as they would be anticipated to reside and associate within the water channels rather than being incorporated within the lipophilic bilayer of the cubic LC structure. This would otherwise likely cause a negative curvature in the system resulting in the formation of a hexagonal phase. Such a negative curvature effect on LC structure has previously been observed after incorporation of hydrophobic gold nanorods in PHY cubic phases [14]. Furthermore, the GNP were not expected to escape from the formulation, as the GNP particles (with a diameter of 15 nm) were sufficiently large to be embedded within the

LC compared to the small aqueous channel pore size of the cubic phase (5–10 nm in diameter) [15]. Therefore, with GNP premixed into the lipid as done here, it was anticipated that the GNP would become trapped in the LC matrix once the lipid swelled and formed the cubic phase in the stomach, resulting in minimal diffusion and separation from the vehicle.

Comparing X-ray micro-CT imaging to analytical determination of gastric retention

In previous studies, gastric retention of PHY and GMO was assessed analytically by chromatographic determination of lipid content in the stomach at fixed time points. Overall, a general correlation was observed between both X-ray micro-CT imaging and previous studies using analytical approaches, where substantial amounts of PHY remained in the stomach after 8 h, compared to the level of GMO which had substantially decreased. Although previous analytical methods provided less variable results, X-ray micro-CT imaging dramatically reduced the number of animals required, whilst providing a non-invasive, and less labour-intensive means of assessing gastric retention of oral formulations in rats.

An additional application of X-ray CT may be in assessing the disposition of formulation in other parts of the GIT than the stomach—in the current study, contrast was also observed from the region of the caecum. The amount of contrast accumulated in the caecum after 8 h for GMO formulation was higher than that for the PHY formulation (Fig 9), suggesting that the formulation had passed more rapidly through the GIT and that the use of GNP as a contrast agent in lipid formulations may also be applied to whole GIT disposition studies, rather than just the gastric compartment which was the focus of the current study.

Combining digestible and non-digestible lipids in formulations can maximise drug absorption

Currently, cinnarizine is available as a tablet dosage form with classical excipients used to prevent motion [16] sickness or to

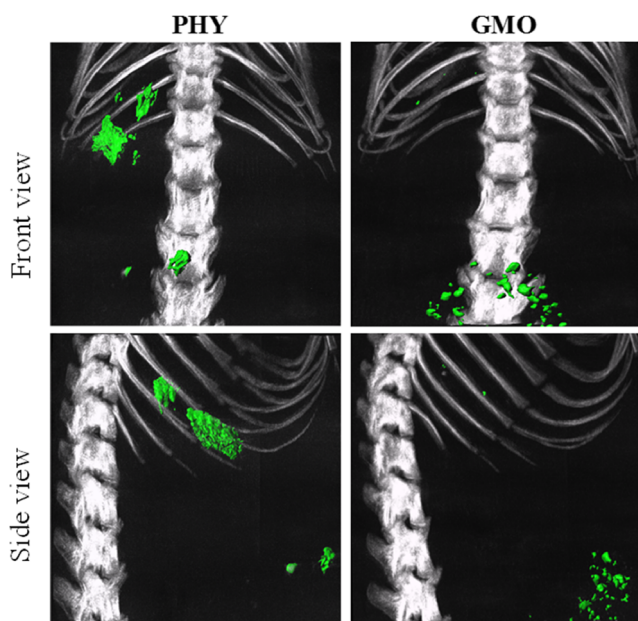


Fig. 9 X-ray CT images of the front (*upper panels*) and side view (*lower panels*) of rats dosed with PHY and GMO containing 5 % w/w GNP, at 8 h after administration, highlighting the lower intestinal content in *the bottom right and lower panels*

treat Ménière's disease [17]. The dose required is high due to it being a poorly water-soluble drug, with adult patients taking up to two tablets three times a day, which can cause variable absorption depending on age [18]. The formulation approach in this study not only focuses on enhancing solubilisation of cinnarizine to improve bioavailability but also to sustain the absorption in order to potentially reduce dosing intervals. Therefore, the combination of GMO and PHY, which was previously demonstrated to increase plasma concentration and sustain absorption of cinnarizine, respectively [2], has proven to exhibit both extremes in this study. The results from the pharmacokinetic studies suggested that balancing an optimal proportion of digestible with non-digestible lipids can allow even greater absorption of the cinnarizine, than digestible or non-digestible lipids alone. Plasma profiles for CZ with combined formulations of PHY with GMO were similar in shape to that for PHY alone, indicating that sustained drug absorption was continuing beyond this time point. This was particularly evident for the 30 % PHY/70 % GMO formulation for which the AUC would likely be substantial. Although time points beyond 24 h were not able to be obtained in this study, a slow return to baseline similar to that previously reported for 100 % PHY [2] could be expected up to 55 h. Therefore, it is hypothesised that CZ absorption from the combined PHY/GMO may be similarly sustained. Furthermore, increases in the proportion of GMO added to PHY greater than 70 %, with pharmacokinetics determined out to 55 h, may provide further optimised mixtures in terms of drug loading and absorption. When the enhanced loading afforded by

the GMO in the optimal mixed systems is also considered, the mixed systems are particularly attractive for improving gastric retention and drug absorption, and further studies in larger species would be particularly interesting.

Influence of lipid digestion on gastric retention and drug absorption

Plasma profiles for CZ from PHY/GMO mixtures provided a synergistic effect in which both sustained absorption relative to 100 % GMO, whilst maintaining plasma concentrations slightly higher than 100 % PHY (Fig. 8). These pharmacokinetic results correlated well with the imaging results, where the mixtures were still retained in the stomach, whereas rapid emptying occurred for the 100 % GMO formulation, evident from the higher accumulation of contrast in the caecum relative to 100 % PHY. The digestibility of GMO is believed to cause the semi-ordered LC structures to breakdown, therefore no longer forming a viscous cubic phase structure upon digestion [2]. This in turn affects gastric retention; however, the digestion products assist with drug absorption. Therefore, increasing the composition of GMO in the mixture correlated generally with increased C_{\max} and decreasing gastric retention. It is well known that drug release from these materials is under diffusion control and depends on surface area; however, the gastric compartment represents a non-sink condition for cinnarizine which leads to the long duration of absorption when the formulation is retained gastrically. In vitro drug release measurements, although common in the literature, are therefore unlikely to provide a useful correlation to the more dynamic in vivo absorption data.

The digestion of GMO mainly within the small intestine liberates oleic acid, which may assist in maintaining the solubilisation of CZ, especially when combined with endogenous solubilising agents in the duodenum [6]. It has also been demonstrated to increase systemic exposure for cinnarizine, enhancing bioavailability when orally dosed in beagles [6]. Interestingly, the generated oleic acid which is then associated with the PHY would then be expected to form a hexagonal phase at pH 2, indicated in the PHY-oleic acid-buffer phase diagram by Du et al. [5]. That is, the incorporation of lipophilic, unionised molecules such as oleic acid into PHY induces a negative curvature to the LC structure, causing phase transition of cubic LC phase to hexagonal LC phase in excess water at specific concentrations. The H_2 phase has also been demonstrated to sustain the absorption of CZ using another non-digestible LC-forming lipid, selachyl alcohol, in excess water [19]. Therefore, these combined mechanisms may explain for the sustained plasma profile with higher C_{\max} from combined PHY/GMO formulations compared to 100 % PHY alone.

Conclusion

A decrease in gastric retention relative to PHY alone but increase in bioavailability was observed when mixtures of PHY and GMO were used as a drug delivery vehicle for poorly water-soluble drugs such as CZ. The use of gold nanoparticles incorporated into the lipid matrix enabled the non-invasive assessment of gastric retention of the formulations, agreeing with previous disposition studies using a larger cohort of animals. Optimised combinations of digestible and non-digestible lipids therefore offer a potential mechanism for enhancing bioavailability of poorly water soluble compounds through modulating sustained drug absorption whilst maintaining higher absorption concentrations. This allows better targeting of drug absorption within the therapeutic window.

Acknowledgments Funding is acknowledged from the Australian Research Council under the Discovery Projects scheme DP120104032. BJB is a recipient of an Australian Research Council Future Fellowship (FT120100697). We acknowledge Tanmay Joshi and Olga Gazukin for transmission electron microscopy (TEM) images, Bim Graham and Raymond Lam for GNP synthesis, Joanne Du and Linda Hong for SAXS analysis and Orlagh Feeney for assistance with UPLC. We also acknowledge the MBI Facility for provision of instrumentation, training and general support. SAXS measurements were performed on the SAXS/WAXS beamline at the Australian Synchrotron facility.

Compliance with ethical standards All institutional and national guidelines for the care and use of laboratory animals were followed.

Conflict of interest The authors declare that they have no competing interests.

References

1. Nguyen T-H, Hanley T, Porter CJH, Boyd BJ. Nanostructured liquid crystalline particles provide long duration sustained-release effect for a poorly water soluble drug after oral administration. *J Control Release*. 2011;153:180–6. **Elsevier B.V.**
2. Nguyen T-H, Hanley T, Porter CJH, Larson I, Boyd BJ. Phytantriol and glyceryl monooleate cubic liquid crystalline phases as sustained-release oral drug delivery systems for poorly water-soluble drugs II. In-vivo evaluation. *J Pharm Pharmacol*. 2010;62:856–65.
3. Boyd BJ, Khoo S-M, Whittaker DV, Davey G, Porter CJH. A lipid-based liquid crystalline matrix that provides sustained release and enhanced oral bioavailability for a model poorly water soluble drug in rats. *Int J Pharm*. 2007;340:52–60.
4. Nielsen LS, Schubert L, Hansen J. Bioadhesive drug delivery systems. I. Characterisation of mucoadhesive properties of systems based on glyceryl mono-oleate and glyceryl monolinoleate. *Eur J Pharm Sci*. 1998;6:231–9.
5. Du JD, Liu Q, Salentinig S, Nguyen T-H, Boyd BJ. A novel approach to enhance the mucoadhesion of lipid drug nanocarriers for improved drug delivery to the buccal mucosa. *Int J Pharm*. 2014;471:358–65.
6. Tokumura T, Tsushima Y, Tatsuishi K, Kayano M, Machida Y, Nagai T. Enhancement of the oral bioavailability of cinnarizine in oleic acid in beagle dogs. *J Pharm Sci*. 1987;76:286–8.
7. Lee KWY, Porter CJH, Boyd BJ. A simple quantitative approach for the determination of long and medium chain lipids in bio-relevant matrices by high performance liquid chromatography with refractive index detection. *AAPS PharmSciTech*. 2013;14:927–34.
8. Connor EE, Mwamuka J, Gole A, Murphy CJ, Wyatt MD. Gold nanoparticles are taken up by human cells but do not cause acute cytotoxicity. *Small*. 2005;1:325–7.
9. Jackson PA, Rahman WNW, Wong CJ, Ackerly T, Geso M. Potential dependent superiority of gold nanoparticles in comparison to iodinated contrast agents. *Eur J Radiol*. 2010;75:104–9. **Elsevier Ireland Ltd.**
10. Clogston J, Rathman J, Tomasko D, Walker H, Caffrey M. Phase behavior of a monoacylglycerol: (myverol 18-99K)/water system. *Chem Phys Lipids*. 2000;107:191–220.
11. Kirby NM, Mudie ST, Hawley AM, Cookson DJ, Mertens HDT, Cowieson N, et al. A low-background-intensity focusing small-angle X-ray scattering undulator beamline. *J Appl Crystallogr*. 2013;46:1670–80. **International Union of Crystallography.**
12. Hyde ST. Identification of lyotropic liquid crystalline mesophases. In: Holmberg K, editor. *Handbook applied surface and colloid chemistry*. New York: John Wiley & Sons, Ltd; 2001. p. 299–332.
13. Du JD, Fong W-K, Salentinig S, Caliph SM, Hawley A, Boyd BJ. Phospholipid-based self-assembled mesophase systems for light-activated drug delivery. *Phys Chem Chem Phys*. 2015;17:14021–7. **Royal Society of Chemistry.**
14. Fong W-K, Hanley TL, Thierry B, Kirby N, Waddington LJ, Boyd BJ. Controlling the nanostructure of gold nanorod-lyotropic liquid-crystalline hybrid materials using near-infrared laser irradiation. *Langmuir*. 2012;28:14450–60.
15. Bhosale RR, Osmani RA, Harkare BR, Ghodake PP. Review article cubosomes: the inimitable nanoparticulate drug carriers. *Sch Acad J Pharm*. 2013;2:481–6.
16. Doweck I, Gordon CR, Spitzer O, Melamed Y, Shupak A. Effect of cinnarizine in the prevention of seasickness. *Aviat Space Environ Med*. 1994;65:606–9.
17. Arab SF, Düwel P, Jüngling E, Westhofen M, Lückhoff A. Inhibition of voltage-gated calcium currents in type II vestibular hair cells by cinnarizine. *Naunyn Schmiedebergs Arch Pharmacol*. 2004;369:570–5.
18. Nowacka-Krukowska H, Rakowska M, Neubart K, Kobylińska M. High-performance liquid chromatographic assay for cinnarizine in human plasma. *Acta Pol Pharm*. 2007;64:407–11.
19. Nguyen T-H, Hanley T, Porter CJH, Boyd BJ. Nanostructured reverse hexagonal liquid crystals sustain plasma concentrations for a poorly water-soluble drug after oral administration. *Drug Deliv Transl Res*. 2011;1:429–38.